

УДК 551.464.3

© A. S. Malysheva^{1,2*}, I. V. Radchenko¹, D. V. Pozdnyakov¹⁻³, 2023

¹Nansen International Environmental and Remote Sensing Centre, 7 14th Line V.O., St. Petersburg, 199034, Russia

²St. Petersburg State University, 7–9 Universitetskaya Emb., St. Petersburg, 199034, Russia

³Karelian Research Centre of the Russian Academy of Sciences, 11 Pushkinskaya Str., Petrozavodsk, 185910, Russia

*alexandra.malysheva@niersc.spb.ru

ARCTIC OCEAN ACIDIFICATION DYNAMICS DURING 1993–2021 AND ITS PROJECTIONS FOR THE REST OF THIS CENTURY

Received 15.03.2023, Revised 11.08.2023, Accepted 24.08.2023

Abstract

Dynamics of acidification of the Arctic Ocean through 1993–2021 and predictions of further tendencies of this process until the end of 2100 were assessed making use of both the GLODAPv.2021 and the Global Ocean Biogeochemistry Hindcast (GOBH) reanalysis data on pH. The projections of pH were performed by CMIP6 models for four scenarios of rates of socio-economic and agricultural development and emissions of greenhouse gases: SSP1–2.6, SSP2–4.5, SSP3–7.0 and SSP5–8.5.

The tendencies of pH decline over the last 27 years (1993–2019) as determined from the GLODAP in situ and the reanalysis data over 1993–2021 proved to be, respectively –0.9% (from 8.18–8.11) and –0.7% (from 8.10–8.05). Thus, the annual acidification rate as assessed from both data sources proved to be –0.03%.

Through the percentile method-based comparison of consistency of historical observation data on pH with GBH model hindcast four best models were identified: MPI-ESM1–2-LR, NorESM2-MM, NorESM2-LM, and CMCC-ESM2. The projection results strongly indicate that the Arctic Ocean acidification will continue till the end of this century. The highest rates of pH decrease (–4.9% and –6.2%) were forecasted, respectively, for scenarios SSP3–7.0 and SSP5–8.5 that implied the global mean temperature increases by 3.6 °C and 4.4 °C, respectively. A comparison of the results obtained with the previously made assessments is indicative that by the end of the current century the rate of acidification (i.e. pH decrease) in the Arctic should be expected to be higher than that averaged over the World Oceans: the difference for each of the SSP scenarios proved to be –0.1.

Keywords: Arctic Ocean, water acidification drivers, past and ongoing dynamics of pH, in situ GLODAP data, reanalysis data, CMIP6 model simulations, acidification hindcast and projections for 2100

© A. S. Мальшева^{1,2*}, Ю. В. Радченко¹, Д. В. Поздняков¹⁻³, 2023

¹Научный фонд «Международный центр по окружающей среде и дистанционному зондированию имени Нансена», 199034, Санкт-Петербург, 14-я Линия В.О., д. 7

²Санкт-Петербургский государственный университет, 199034, Санкт-Петербург, Университетская наб., д. 7–9

³Карельский научный центр Российской академии наук, 185910, Петрозаводск, ул. Пушкинская, д. 11

*alexandra.malysheva@niersc.spb.ru

ДИНАМИКА ПОДКИСЛЕНИЯ СЕВЕРНОГО ЛЕДОВИТОГО ОКЕАНА В 1993–2021 ГГ. И ЕЕ ПРОГНОЗ НА КОНЕЦ 21-ГО ВЕКА

Статья поступила в редакцию 15.03.2023, после доработки 11.08.2023, принята в печать 24.08.2023

Аннотация

С использованием данных GLODAP v.2021 и реанализа Global Ocean Biogeochemistry Hindcast GOBH по параметру pH проведены численные оценки динамики подкисления вод Арктического региона (60–90° с.ш.) за период 1993–2021 гг. и выявлены тенденции подкисления океана (ПО) в свете проекций климата Арктики до конца 2100 года. Будущие тенденции ПО были рассчитаны по моделям CMIP6 для четырех сценариев Shared Socioeconomic Pathways (SSP), в которых представлены разные уровни социально-экономического и сельскохозяйственного развития и эмиссии парниковых газов: SSP1–2.6, SSP2–4.5, SSP3–7.0 и SSP5–8.5.

Ссылка для цитирования: Мальшева А.С., Радченко Ю.В., Поздняков Д.В. Динамика подкисления Северного Ледовитого океана в 1993–2021 гг. и ее прогноз на конец 21-го века // *Фундаментальная и прикладная гидрофизика*. 2023. Т. 16, № 4. С. 63–74. doi:10.59887/2073-6673.2023.16(4)-5

For citation: Malysheva A.S., Radchenko I.V., Pozdnyakov D.V. Arctic Ocean acidification dynamics during 1993–2021 and its projections for the rest of this century. *Fundamental and Applied Hydrophysics*. 2023, 16, 4, 63–74. doi:10.59887/2073-6673.2023.16(4)-5

Тенденции снижения pH, определенные по *in situ* данным GLODAP за период 1993–2019 гг. и по данным реанализа за 1993–2021 гг., составили, соответственно: $-0,9\%$ (от 8,18–8,11) и $-0,7\%$ (от 8,10–8,05). Таким образом, годовая скорость подкисления, оцененная по обоим источникам данных, составила $-0,03\%$.

На основе метода перцентилей сравнены исторические сценарии pH моделей CMIP6 с данными реанализа, и на этой базе установлены четыре лучшие модели: MPI-ESM1-2-LR, NorESM2-MM, NorESM2-LM и CMCC-ESM2. Результаты прогнозирования указывают на то, что подкисление вод Арктики будет продолжаться до конца этого столетия. Наибольшие темпы снижения pH ($-4,9\%$ и $-6,2\%$) соответствуют сценариям SSP3-7.0 и SSP5-8.5, предполагающих повышение средней глобальной температуры на $3,6\text{ }^{\circ}\text{C}$ и $4,4\text{ }^{\circ}\text{C}$ соответственно. Сопоставление полученных результатов с численными оценками динамики pH других авторов свидетельствует, что к концу текущего столетия скорость подкисления (т.е. снижения pH) в Арктике следует ожидать выше, чем в среднем по Мировому океану: разница между каждым из SSP сценариев оказалась равной $-0,1$.

Ключевые слова: Северный Ледовитый океан, факторы подкисления воды, историческая и текущая динамика pH, *in situ* GLODAP data, реанализ, модели CMIP6, прогноз подкисления и проекции на 2100 г.

1. Introduction

The World's oceans (WO) are the main sink for atmospheric CO_2 . An increase in atmospheric CO_2 concentration alters the balance between the partial pressure of CO_2 ($p\text{CO}_2$) at the ocean-atmosphere interface, increasing the flow of CO_2 into the ocean. Dissolved CO_2 interacts with water molecules to form carbonic acid, which dissociates into bicarbonates (HCO_3^{2-}) and free hydrogen ions [H^+] [1]. The enhancement of [H^+] concentration implies acidification of the environment, i. e., a decline in pH over decades or longer time periods [2].

Sources of increased CO_2 in the atmosphere primarily include anthropogenic activities such as burning fossil fuels (coal, oil, natural gas), deforestation, and chemistry-based land use practices. In addition, many natural sources, such as volcanic eruptions, decomposition of wood processing waste, and increased liberation and ensuing mineralization of soil organic matter under conditions of global warming contribute significantly [3].

In addition to increased flux of CO_2 from the atmosphere, other physical and biogeochemical processes influence the dynamics of ocean acidification (OA) among which are 1. photosynthesis of marine phytoplankton, during which enormous amounts of atmospheric CO_2 are fixed annually, 2. biological mineralization of both organic matter (including its dissolved fraction) and dead organisms; 3. remineralization in coastal surface waters of organic carbon from land runoff, 4. melting of sea ice, 5. vertical mixing due to strong wind action, 6–7. enhanced Ekman transport and upwelling. Combined with increased anthropogenic CO_2 , all of the above factors/processes continuously condition the level of OA [4–7].

Significant acidification of seawater can cause major changes in the ocean carbonate system, affecting the partial pressure of dissolved CO_2 , $p\text{CO}_2$, concentration of dissolved inorganic matter, levels of pH and alkalinity, and CaCO_3 saturation state [8]. In combination with global warming that drives a global decline of dissolved oxygen in the ocean, referred to as ocean deoxygenation, because of warming-induced reduction in O_2 solubility, increased stratification and reduced ventilation [9, 10], OA is liable to cause changes in metabolism in marine organisms as well as alterations of biogeochemical cycles, changes in ecosystems and their interactions [11]. In the case of calcifying organisms, a marked slowdown is observed in their calcification rates driven by a chain of consequential chemical responses: increase in $p\text{CO}_2$, ensuing decrease in pH and reduction of carbonate ion concentration, CO_3^{2-} [12]. Due to OA enhancement, ion exchange in bony fish and marine invertebrates is reportedly reduced, inhibiting protein synthesis and causing metabolic rate lowering [13]. Under more acidic conditions, physiological and behavioral functions of living organisms are allegedly impaired [14].

The reconstruction of the historical chronicles testifies to OA events that occurred in the early geological epochs. The most significant event occurred during the Paleocene-Eocene Thermal Maximum [PETM — Paleocene-Eocene Thermal Maximum] [15], which resulted in a catastrophic disruption of the carbon cycle and cardinal changes in the climatic status on a planetary scale. It has been estimated that over the past 10,000 years, surface water pH was 8.2 and varied by less than ~ 0.04 [16]. Remarkably, pH was 0.1–0.2 units higher during glacial periods than during interglacial periods.

As noted above, OA processes are closely related to the variability of atmospheric CO_2 concentrations, which have increased since the pre-industrial epoch, from 280 parts per million (ppm) to 380 ppm at the beginning of the 21st century [17]. It was a huge increase over the last 20,000 years (since the peak of the last ice age). By the middle of the 21st century, atmospheric CO_2 levels could reach 500 ppm and even exceed 800 ppm by the end of the century [17]. Predicted high CO_2 concentrations are expected to lower the pH level of the world's surface ocean waters by the end of 2100 by 0.3 units compared to current conditions and by 0.4 units compared to pre-industrial conditions. Such changes imply a 2.5-fold enhancement of hydrogen ion concentration, [H^+] in the ocean compared to the beginning of the industrial era [18].

The average pH of surface waters in the WO ranges from 7.9 to 8.3, i. e. seawater is a slightly alkaline solution [19]. Counting for the time period 1800–1994, the WO waters have absorbed about 30 % of anthropogenic carbon emissions [20]. This resulted in pH decrease in global surface water of about 0.1 (8.25 to 8.14) [17, 21], which corresponds to a nearly 30 % increase in $[H^+]$ [17]. As in the early 2000s, pH was ~ 8.069 , corresponding to a ~ 28.8 % decrease relative to the pre-industrial era [17].

It is found that in high latitudes, the rate of OA is twice as fast as in the tropics and subtropics [18]. In the Arctic, OA is thought to be enhanced by low water temperatures, increased freshwater storage (river runoff and ice melt), and influx of low pH Pacific waters [22]. In addition, in coastal areas, which is especially characteristic of the Laptev Sea, the East Siberian and Chukchi Seas, high concentrations of CO_2 are the result of the aforementioned process of decomposition of allochthonic organic matter that is carried out in large amounts with river waters [22].

In light of the above, it was of interest to (i) numerically assess the contemporary (1993–2021) dynamics of acidification of the Arctic Ocean (AO) as an area of particularly significant climate warming — the so-called Arctic acceleration phenomenon [23] and (ii) to analyze future OA trends in light of climate change projections for the current century. The results of these investigations are reported in the present paper.

2. Data sources for this study and their characteristics

In situ data from the GLODAPv2.2021 (Global Ocean Data Analysis Project) database [24], were used. Estimates of pH, water temperature [$^{\circ}C$], and chlorophyll-*a* concentration [$mg\ m^{-3}$] were taken from 1993 to 2019 at 4,970 stations in the surface horizon (0–20 m). The stated accuracy of the pH data is 0.005. The pH values are referenced to a common scale from in situ water temperature and atmospheric pressure data. The data are not interpolated on a regular grid.

The main part of measurements was from May to October. The greatest number of measurements was carried out in the warm period of the year when the ice-free area is maximal: in July (879 stations out of 4970), August (1326 stations out of 4970) and September (1180 stations out of 4970). These stations are located in the central part of the Arctic, as well as in the North Atlantic, the Beaufort Sea, the Bering Strait, the Laptev and the East Siberian Seas. From October to May there are data on the stations predominantly located in the Greenland and Norwegian Seas.

It was found that the range of pH values according to the GLODAP database was from 6.97 to 9.35, with an average value of 8.14 ± 0.13 . The distribution of pH values appeared to be close to normal (Fig. 1, *a*).

The spatial distribution of pH in the AO is characterized by considerable heterogeneity (Fig. 2, *a*). In the deltas of both large and some less high-flowing Siberian rivers (Ob, Yenisei, Lena, Kolyma, Palyavaam, Anadyr) pH values drop drastically down (to 7.8 and even 7.7), which determines the acidification of vast seas such as the Laptev and the

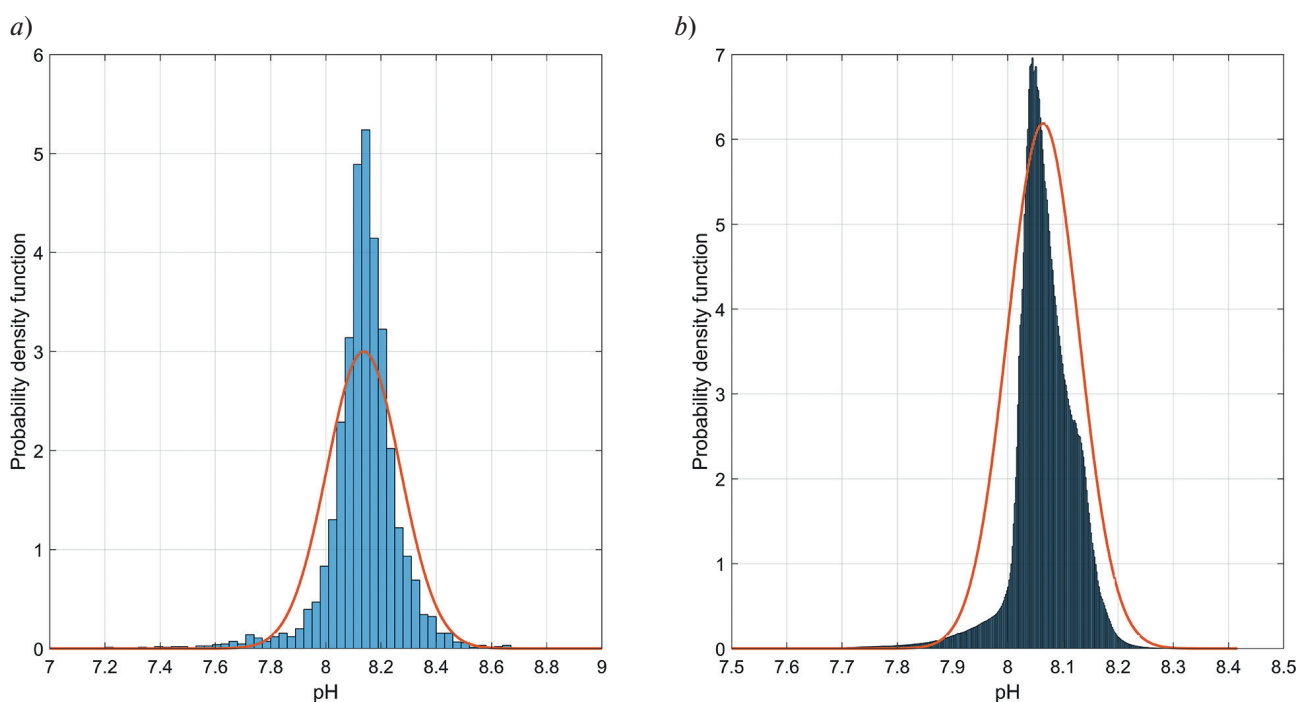


Fig. 1. AO: Distribution of probability density of pH values according to: *a* — the GLODAP data ($n = 4970$); *b* — the reanalysis data ($n = 60635520$). Brown line = normal distribution; pH scale is given as a colour bar

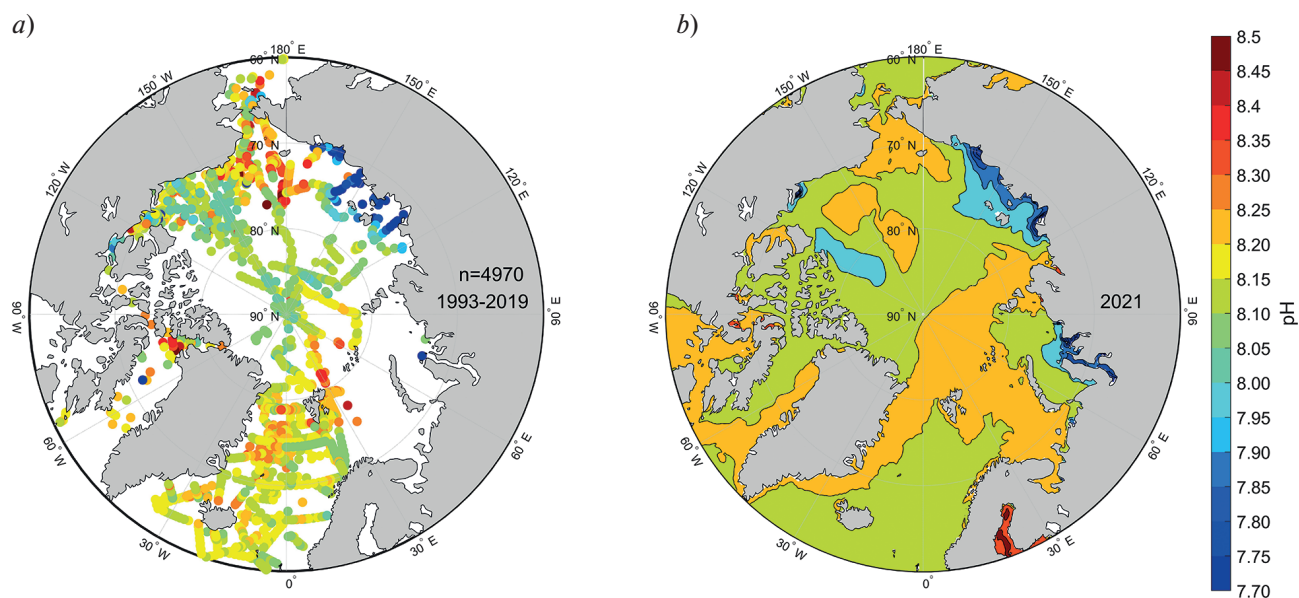


Fig. 2. Spatial distribution of: *a* — GLODAP station locations and their determined pH values for the period 1993–2019; *b* — mean pH values from the reanalysis data for 2021; pH scale for both datasets is given as a colour bar

East Siberian Seas, as well as locally the Bering Sea (Fig. 2, *a*). As noted in the Introduction section, acidification in these areas is the result of biochemical (partly photochemical) oxidation/mineralization of dissolved organic matter, which Siberian riverine waters are rich in due to the presence of vast ranges of soils with high humus content in their catchment areas [25, 26]. A similar explanation can be given for the existence of more acidified areas of the AO water area in the Canadian shelf zone influenced by the Mackenzie River runoff.

Values above the mean (more than 8.1) are characteristic of waters in the Northern AO in the area of the Spitsbergen Archipelago and Iceland (zones of outlet of deep and, therefore, less acidified waters as they were not exposed to the increasing input of CO₂ from the atmosphere) as well as in the Bering Sea. Another pH-enhanced part of the AO is the extensive area of inflow of the Pacific water into the AO through the Bering Strait, where the maximum pH values (more than 8.3) are recorded [27].

Given that only model simulations permit to prognose AO acidification trends for the future up to the end of the 21st century, we used CMIP6 models. Implementation of this approach requires a preliminary selection of models from the CMIP6 pool, based on the timeseries of input parameters, including pH, for the so-called historical/reference time period. This requires continuous timeseries of monthly averaged pH variations across the AO over the reference period. Not available from the GLODAP database, such monthly timeseries were obtained from the Global Ocean Biogeochemistry Hindcast, GOBH (GLOBAL_MULTIYEAR_BGC_001_029) reanalysis data [28].

The carbonate system model of this product takes data from GLODAPv2 as initial conditions. The spatial resolution of the data is 0.25° × 0.25°, the temporal resolution is one month. Exclusively subsurface (–0.5 m) data were considered, and the reference period was taken from 1993 to 2021.

The spatial distribution of pH values in the reanalysis database is also characterized by high variability (Fig. 2, *b*) whose pattern appreciably differ from that in the GLODAP field data, while still respecting the major common features such as the presence and location of extensive zones of elevated and low pH values (Fig. 2).

Numerically, the reprocessed pH data from both the above-mentioned areas, and generally across the entire AO, also differ from that provided by GLODAP. The same refers to the probability density curve of pH values according to the reanalysis data: it is clearly two-modal in contrast to the monomodal distribution of the pH data from GLODAP (Fig. 1, *b*). The peak of the first mode does not coincide with the peak of normal distribution and the peak of the second mode can be traced at pH = 8.15. For the time period considered, the mean pH value from the reanalysis and GLODAP databases also differ constituting 8.06 ± 0.01 and 8.14 ± 0.13, respectively. The range of pH values from the reanalysis data is from 6.01 to 8.40, which is lower than that of GLODAP (Table 1).

The revealed inconsistencies in the GLODAP and reanalysis databases necessitated some objective assessment of appropriateness of using the GOBH data for the present study. The GLODAP and reanalysis data were compared for stations with strictly the same date and coordinates as close as ±1 km. The comparison shows that the reanalysis data describe 62% of the GLODAP (i. e. in situ) data ($r^2 = 0.62$, $p < 0.01$, $N = 56$). The comparison results argue for the validity of using reanalysis data to predict pH dynamics by the end of 2100 using CMIP6 models.

Table 1

Comparison of pH time series characteristics for the reference period (1993–2019) according to the GLODAP and GOBH data

Parameters	GLODAP	GOBH
Minimal value of pH	6.97	6.01
Maximal value of pH	9.37	8.42
Average value of pH	8.14±0.13	8.06±0.01
Acidification tendency	–0.9 %	–0.7 %
Acidification rate	–0.03 % per year	–0.03 % per year

3. Results and discussion

3.1. Water acidity dynamics in the AO over the time period 1993–2021

Assessment of the dynamics of AO water acidification using the GLODAP (i. e. in situ) data shows that over 27 years (from 1993 to 2019), the AO average pH value decreased by 0.9 % from 8.18 to 8.11 (Fig. 3). The overall feature is increasing acidification. However, there were cases of pH growth up to 8.20 throughout the above time period, specifically in 1995 and 2005. Contrarily, the lowest pH value occurred in 2010 and constituted 8.03. The rate of acidification proved to be –0.03 % per year.

According to the reanalysis products employed, the interannual ocean-mean pH values fluctuated only weakly during 1993–2021 (Fig. 3): from 8.10 to 8.05, and the acidification trend constituted –0.7 % over the above time period with the rate of acidification equal to –0.03 % per year.

The above results illustrate the general consistency between the two sources of data on pH temporal changes spatially averaged over the AO, and therefore provide additional albeit still cautious, support for the validity of using pH trends from the reanalysis data over the reference time period for CMIP6 predictions.

3.2. Assessment of future tendencies of the AO acidification throughout the rest of the current century

To calculate future trends in OA for the Arctic region (60–90°N), the atmosphere–ocean general circulation models (GCMs) of the international CMIP6 project (Phase 6 of the Coupled Model Intercomparison Project) were used.

The assessment of OA was performed based on the variability of pH. In the CMIP6 project, this parameter is calculated in 12 models (Table 2). For the present task, monthly-averaged pH values from the Earth System Grid Federation portal [29] were taken.

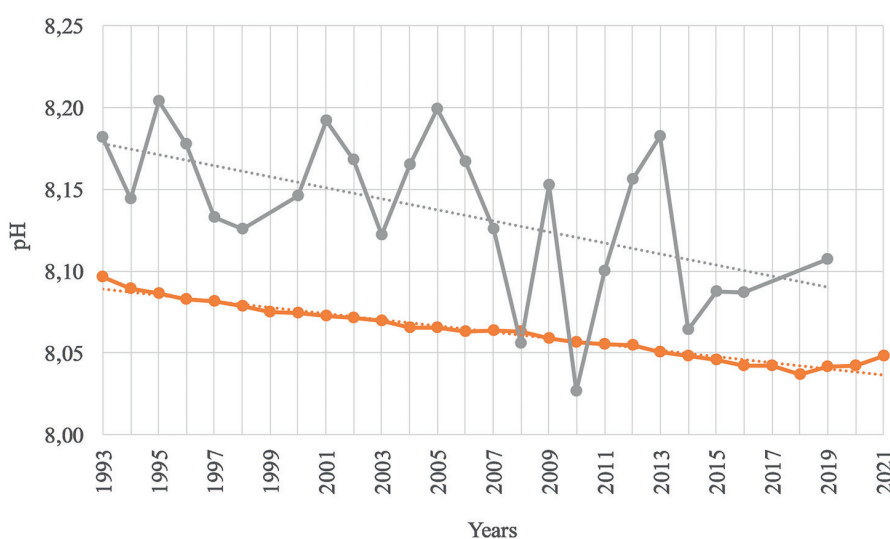


Fig. 3. Interannual variability of AO acidification: across 1993–2019 as revealed from GLODAP data — grey line; during 1993–2021 according to reanalysis data — brown line; dotted lines — trend lines. Linear regression equation according to GLODAP data: $y = -0.003x + 8.18$, $r^2 = 0.29$. Linear regression equation according to reanalysis data: $y = -0.002x + 8.09$, $r^2 = 0.96$

Table 2

List of both global climate models of the international CMIP6 project that simulate pH projections and simulations. Historical simulations were made over 1990–2014, the SSP scenarios are designed for the time period 2015–2100

Model	Model Developer	Grid, km	Simulations
CESM2-FV2	National Center for Atmospheric Research, Geophysical Fluid Dynamics Laboratory, USA	320 × 384	Historical
CMCC-ESM2	Euro-Mediterranean Center on Climate Change, Italy	362 × 292	Historical, SSP1–2.6, SSP2–4.5, SSP3–7.0, SSP5–8.5
GFDL-CM4	National Oceanic and Atmospheric Administration, Geophysical Fluid Dynamics Laboratory, USA	360 × 180	SSP2–4.5, SSP5–8.5
GFDL-ESM4			Historical, SSP1–2.6, SSP2–4.5, SSP3–7.0
IPSL-CM5A2-INCA	Pierre-Simon Laplace Institute, France	362 × 332	Historical
IPSL-CM6A-LR			Historical, SSP1–2.6, SSP2–4.5, SSP3–7.0
IPSL-CM6A-LR-INCA			Historical
MPI-ESM-1-2-HAM	Max Planck Institute for Meteorology — MPI-M	256 × 220	Historical
MPI-ESM1-2-HR		802 × 404	Historical
MPI-ESM1-2-LR		256 × 220	Historical, SSP1–2.6, SSP2–4.5, SSP3–7.0, SSP5–8.5
NorESM2-LM	The NorESM climate modeling consortium, consisting of CICERO (Center for International Climate and Environmental Research, Oslo), MET-Norway (Norwegian Meteorological Institute, Oslo), NERSC (Nansen Environmental and Remote Sensing Center, Bergen), NILU (Norwegian Air Research Institute, Hjeller), UiB (University of Bergen, Bergen), UiO (Oslo University, Oslo) and UNI (Research Institute, Bergen), Norway.	360 × 384	Historical, SSP1–2.6, SSP2–4.5, SSP3–7.0, SSP5–8.5
NorESM2-MM			Historical, SSP1–2.6, SSP2–4.5, SSP3–7.0, SSP5–8.5

As mentioned above, to perform pH simulations by CMIP6 climate models, the GOBH [28], reanalysis products were used a proxy for observed point data on pH.

Five SSP (Shared Socioeconomic Pathways) possible scenarios were used to generate projections of the Arctic OA future tendencies according to CMIP6 global climate models, in which different levels of socio-economic development, greenhouse gas emissions into the atmosphere, land use development and radiation impact are presented (Table 3).

Within the CMIP6 pool, there are 12 pH models available for the historical/reference period. However, at the moment of our study, there were no freely available pH models for SSP1–1.9. As to the rest models, 6, 7, 6 and 5 pH models were available for SSP1–2.6, SSP2–4.5, SSP3–7.0, and SSP5–8.5 scenarios, respectively (Table 2).

The performance of the above pH models was assessed using the method of percentiles [32] for the entire AO. This approach analyses the mean spatially-averaged climatology of the inter- and interannual variability of pH in the AO using the following statistical measures: (i) correlation coefficient (*r*), (ii) root mean square error (RMSE), (iii) standard deviation (STD), (iv) climate prediction index (CPI: the ratio of RMSE to STD of observational data), (v) the spatial distribution of temporal trends as well as (vi) spatial bias between the model data and reanalysis for the analysis of interannual variability. Amplitude values of the statistical measures are further used for their grouping into 4 categories: less than 25th percentile — very good, 25th–50th — good, 50th–75th — satisfactory, more than 75th percentile — unsatisfactory. To each group a score from 3 to 0 is assigned, respectively. The group with very good

Table 3

Description of 5 possible future SSP scenarios by O'Neill et al., 2016; IPCC, 2021 [30, 31]

Parameter	SSP1–1.9	SSP1–2.6	SSP2–4.5	SSP3–7.0	SSP5–8.5
Solar radiation impact, W/m ²	1.9	2.6	4.5	7.0	8.5
Level of greenhouse gas emissions	Zero CO ₂ emissions by 2050	Zero CO ₂ emissions by 2080	Slow reduction of CO ₂ emissions by 2100	Increased CO ₂ emissions by 2100	High CO ₂ emissions
Increase in average air temperature by 2100, °C	1.4	1.8	2.7	3.6	4.4

and unsatisfactory model results is assigned to $r > 0.75$ and < 0.25 , respectively. Scores of each statistical measure are then summed up to obtain the model-specific total skill score. Finally, based on this total skill score, the models are ranked, and the top 25% of the examined climate models compose the pH sub-ensemble. Table 4 illustrates the results of performance of the selected CMIP6 pH models.

At the next stage, the best pH models were selected, and their number proved to be 4 (Table 4). Given that two pH models with maximum scores (IPSL–CM5A2-INCA and MPI-ESM-1–2-HAM) have no data on SSP scenarios (Table 2), next 4 pH models (Table 4) were included in the subset of models (To comply with the top-25 model approach, it is generally necessary to probe one quarter of the considered set of 12 models i. e. 3 models; however, instead of 3 we had to employ 4 models as both the 3rd and 4th models showed one and the same threshold score (29)).

In the final sub-ensemble of pH models (Table 4) the best proved to be MPI-ESM1–2-LR: 30 scores. Besides it, the best results in pH modeling are shown by: NorESM2-MM, NorESM2-LM, and CMCC-ESM2. The least representative models are: GFDL–CM4, GFDL-ESM4 (Table 4).

As Fig. 4 illustrates, over the 1993–2014 reference period, the pH data from the reanalysis do not coincide with the pH data from the CMIP6 multi-model ensemble. However, the reanalysis pH data are within the uncertainty range (25–75 percentile) of the CMIP6 modeled data. At the point of link-up (i. e. 2015) of the pH data produced for the reference period by the sub-ensemble of models with the results of projections emerging from the future scenarios, the average pH values coincided (Fig. 4).

According to the CMIP6 model projections, pH by the end of the 21st century will be 7.98 in the case of SSP1–2.6 scenario, the AO trend as compared to the average in situ pH value from the GLODAP database for 2019 is -1.4% (Table 5). In the case of SSP2–4.5 scenario, by 2100 pH will be 7.86 (trend -2.9%). Under SSP3, pH will be in the range 7.0–7.71 (trend -4.9%) and under SSP5, pH will be within 8.5–7.71 and the trend will be as high as -6.2% .

When using all available models in the ensemble with four SSP scenarios, the range of uncertainty increases. At the point of link-in of the time series in 2015, there is a clear mismatch in the average model pH values (Fig. 5), which indicates that the method of best model selection is correct.

Thus, modeling predictions based on employment of the top four models sub-ensemble results in a 0.1–0.2% decrease of the AO acidification rate as compared with the predictions utilizing the sub-ensemble comprising all available models under SSP scenarios. At the point of link-in of the time series in 2015, there is a clear mismatch in the average model pH values (Fig. 5), which indicates that the method of best model selection is correct. Comparison of our results with the estimates reported elsewhere [31] reveals that the acidification rate in the AO will be more significant than that averaged over the entire WO (Fig. 4 and Fig. 6): the difference for each of the SSP scenarios is -0.1 . In light of the immediately above, it can be only emphasized that in comparison with the approach utilizing the sub-ensemble comprising all available models under SSP scenarios, the employment of the best models selection approach permits to quantify and regionalize the acidification rate more accurately.

Table 4

Ranked list of CMIP6 pH models based on total skill scores. Selected sub-ensemble of AO climatic pH models (4) available for four SSP scenarios is highlighted in grey colour

№	pH Models	Scores	SSP1–2.6	SSP2–4.5	SSP3–7.0	SSP5–8.5
1	IPSL–CM5A2-INCA	34	–	–	–	–
2	MPI-ESM-1–2-HAM	31	–	–	–	–
3	MPI-ESM1–2-LR	30	+	+	+	+
4	NorESM2-MM	30	+	+	+	+
5	NorESM2-LM	29	+	+	+	+
6	CMCC-ESM2	29	+	+	+	+
7	IPSL–CM6A-LR	26	+	+	+	–
8	IPSL–CM6A-LR-INCA	25	–	–	–	–
9	CESM2-FV2	23	–	–	–	–
10	MPI-ESM1–2-HR	23	–	–	–	–
11	GFDL-ESM4	15	+	+	+	–
12	GFDL–CM4	6	–	+	–	+

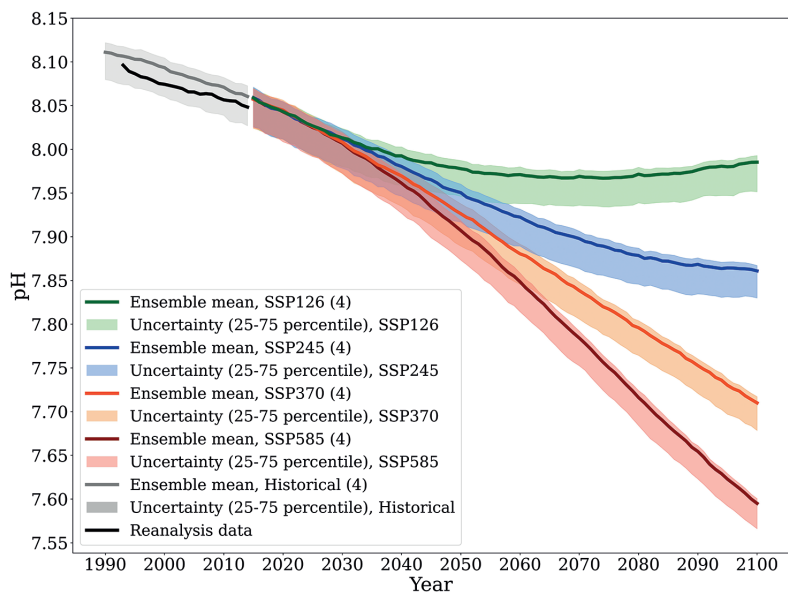


Fig. 4. Projections of pH dynamics in the AO as obtained from application of the sub-ensemble of the top 4 pH models

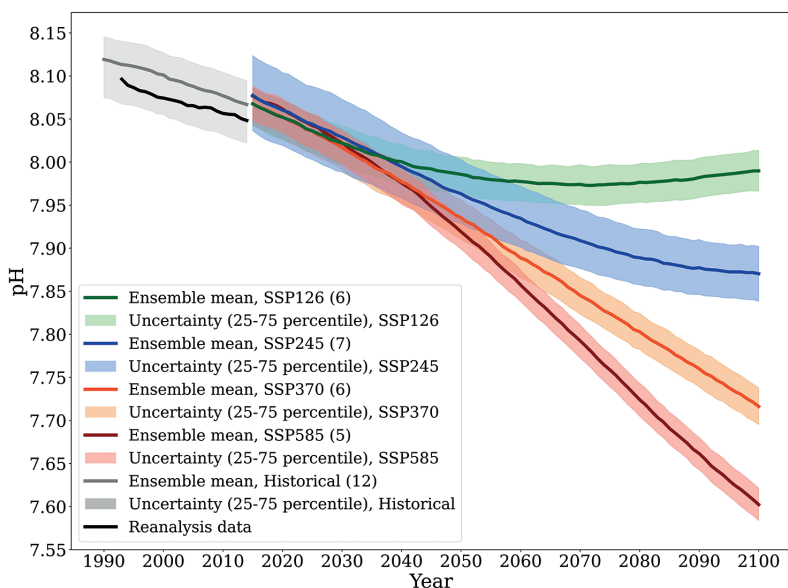


Fig. 5. Four SSP scenario-based predictions of the AO acidification: ensemble of all available pH models

Table 5

Prediction of AO waters acidification according to the exploited scenarios with the application of the sub-ensemble comprising the top four models and the sub-ensemble comprising all available models. Tendency over 2019–2100 was calculated relative to the value of pH at ~8.10 as per 2019 (GLODAP in situ data)

Scenario	Sub-ensemble comprising the top four models		Sub-ensemble comprising all available models	
	pH by 2100	Tendency over 2019–2100	pH by 2100	Tendency over 2019–2100
SSP1–2.6	7.98	–1.4%	7.99	–1.4%
SSP2–4.5	7.86	–2.9%	7.87	–2.8%
SSP3–7.0	7.71	–4.9%	7.72	–4.7%
SSP5–8.5	7.59	–6.2%	7.60	–6.1%

4. Conclusions

Based on our analysis of the GLODAP data relating to the time period 1991–2019, we determined a decrease in pH in the AO by 0.9%, which corresponds to a rate of -0.03% /year; the same annual rate of acidification is found from processing the employed reanalysis data.

Assessed from the simulations performed by carefully selected sub-ensemble of CMIP6 models (MPI-ESM1-2-LR, NorESM2-MM, CMCC-ESM2, NorESM2-LM), the AO acidification by the end of the 21st century is expected to continue.

The highest rates of acidification (-4.9% and -6.2%) are predicted, respectively, under SSP3-7.0 and SSP5-8.5, in which the global average air temperatures in 2100 will rise by $3.6\text{ }^{\circ}\text{C}$ and $4.4\text{ }^{\circ}\text{C}$. If we assign such extremely high rates of atmospheric warming to the category of low confidence, then more realistic rates of AO acidification should be expected in the range -1.4% to -2.9% .

Funding

This study was funded by the Ministry of Science and Higher Education of the Russian Federation under project No. 13.2251.21.0006 (Agreement No. 075-10-2021-104 in the RF “Electronic Budget” System).

Финансирование

Исследование выполнено при финансовой поддержке Министерства науки и высшего образования Российской Федерации по проекту № 13.2251.21.0006 (Соглашение № 075-10-2021-104 в ГИИС «Электронный бюджет»).

References

1. Doney S.C., Fabry V.J., Feely R.A., Kleypas J.A. Ocean Acidification: The other CO₂ problem. *Annual Review of Marine Science*. 2009, 1, 169–192. doi:10.1146/annurev.marine.010908.163834
2. Xue L., Cai W.-J. Total alkalinity minus dissolved inorganic carbon as a proxy for deciphering ocean acidification mechanisms. *Marine Chemistry*. 2020, 222, 103791. doi:10.1016/j.marchem.2020.103791
3. Mostafa K.M.G., Liu C.-Q., Zhai W. et al. Reviews and syntheses: Ocean acidification and its potential impacts on marine ecosystems. *Biogeosciences*. 2016, 13, 1767–1786. doi:10.5194/bg-13-1767-2016
4. Feely R.A., Doney S.C., Cooley S.R. Ocean acidification: Present conditions and future changes in a high-CO₂ world. *Oceanography*. 2009, 22(4), 36–47. doi:10.5670/oceanog.2009.95
5. Salisbury J., Green M.L., Hunt C.W., Campbell J.W. Coastal acidification by rivers: A threat to shellfish? *Eos, Transactions American Geophysical Union*. 2008, 89, 50, 513. doi:10.1029/2008EO500001
6. Yamamoto A., Kawamiya M., Ishida A., Yamanaka Y., Watanabe S. Impact of rapid sea-ice reduction in the Arctic Ocean on the rate of ocean acidification. *Biogeosciences*. 2012, 9, 2365–2375. doi:10.5194/bg-9-2365-2012
7. Yang X., Xue L., Li Y. et al. Treated wastewater changes the export of dissolved inorganic carbon and its isotopic composition and leads to acidification in coastal oceans. *Environmental Science and Technology*. 2018, 52(10), 5590–5599. doi:10.1021/acs.est.8b00273
8. Capelle D.W., Kuzyk Z.A., Papakyriakou T. et al. Effect of terrestrial organic matter on ocean acidification and CO₂ flux in an Arctic shelf sea. *Progress in Oceanography*. 2020, 185, 102319. doi:10.1016/j.pcean.2020.102319
9. Keeling R.F., Körtzinger A., Gruber N. Ocean deoxygenation in a warming world. *Annual Review of Marine Science*. 2010, 2, 1, 199–229. doi:10.1146/annurev.marine.010908.163855
10. Oschlies A., Brandt P., Stramma L., Schmidtko S. Drivers and mechanisms of ocean deoxygenation. *Nature Geoscience*. 2018, 11, 7, 467–473. doi:10.1038/s41561-018-0152-2
11. Riebesell U., Zondervan I., Rost B. et al. Reduced calcification of marine plankton in response to increased atmospheric CO₂. *Nature*. 2000, 407, 364–367. doi:10.1038/35030078
12. Albright R., Caldeira L., Hoffelt J. et al. Reversal of ocean acidification enhances net coral reef calcification. *Nature*. 2016, 531, 362–365. doi:10.1038/nature17155

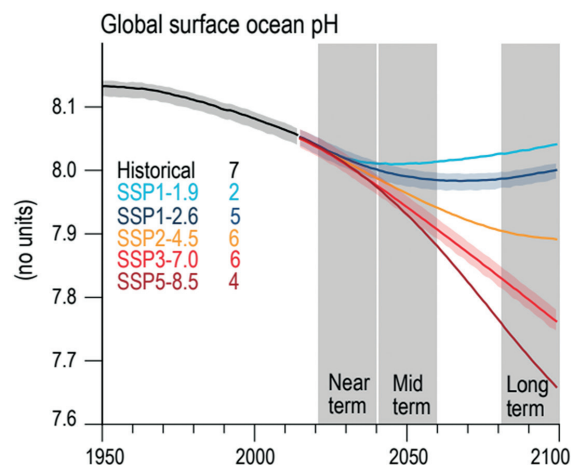


Fig. 6. Five SSP scenario-based predictions of the WO acidification: ensemble of pH models from CMIP6 (Fig. 4.8 IPCC Sixth Assessment Report (AR6) 2021 [31])

13. Pörtner H.-O. Ecosystem effects of ocean acidification in times of ocean warming: A physiologists view. *Marine Ecology Progress Series*. 2008, 373, 203–217. doi:10.3354/meps07768
14. Kwiatkowski L., Torres O., Bopp L. et al. Twenty-first century ocean warming, acidification, deoxygenation, and upper-ocean nutrient and primary production decline from CMIP6 model projections. *Biogeosciences*. 2020, 17, 3439–3470. doi:10.5194/bg-17-3439-2020
15. Zachos J.C., Röhl U., Schellenberg S.A. et al. Rapid acidification of the ocean during the paleocene-eocene thermal maximum. *Science*. 2005, 308, 5728, 1611–1615. doi:10.1126/science.1109004
16. Zeebe R.E., Ridgwell A. Past changes in ocean carbonate chemistry. *Ocean Acidification*. Ed. by Gattuso J.-P. and Hansson L. *Oxford University Press, Oxford*. 2011, 21–40. doi:10.1093/oso/9780199591091.003.0007
17. Raven J., Caldeira K., Elderfield H. et al. Ocean acidification due to increasing atmospheric carbon dioxide. *The Royal Society, London, UK*, 2005. 68 p.
18. Jiang Z., Song Z., Bai Y. et al. Remote sensing of global sea surface pH based on massive underway data and machine learning. *Remote Sensing*. 2022, 14(10), 2366. doi:10.3390/rs14102366
19. Bindoff N.L., Willebrand J., Artale V. et al. Observations: oceanic climate change and sea level. *Climate change 2007: The physical science basis. Contribution of Working Group I / Ed. by: Solomon S., Qin D., Manning M., Chen Z., Marquis M., Averyt K.B., Tignor M., Miller H.L. Cambridge University Press, Cambridge*. 2007, 385–428.
20. Sabine C.L., Feely R.A., Gruber N. et al. The Oceanic Sink for Anthropogenic CO₂. *Science American Association for the Advancement of Science (AAAS)*. 2004, 305, 5682, 367–371. doi:10.1126/science.1097403
21. Orr J.C., Fabry V.J., Aumont O. et al. Anthropogenic ocean acidification over the twenty-first century and its impact on calcifying organisms. *Nature*. 2005, 437, 681–686. doi:10.1038/nature04095
22. Bellerby R., Anderson L., Osborne E. et al. Arctic Ocean Acidification: an update. *AMAP Assessment 2018: Arctic Ocean Acidification. Arctic Monitoring and Assessment Programme (AMAP), Tromsø, Norway*, 2018. 187 p. doi:10.25607/OBP-783
23. Will S. The Arctic in an Earth system context: From brake to accelerator of change. *Ambio*. 2006, 35, 4, 153–159.
24. Lauvset S.K., Lange N., Tanhua T. et al. Global Ocean data analysis project version 2.2021 (GLODAPv2.2021) (NCEI Accession 0237935). NOAA National Centers for Environmental Information. Dataset. 2021. URL: <https://www.ncei.noaa.gov/access/metadata/landing-page/bin/iso?id=gov.noaa.nodc:0237935> (дата обращения: 26.02.2023). doi:10.25921/ttgq-n825
25. Artemiev V.E. Geochemistry of organic matter in the river-sea system. *M., Nauka*, 1993. 204 p. (in Russian).
26. Smirnov M.P. Dissolved organic matters and mineralization of river water of mountains with tundra-taiga types of vertical zoning in Russia. *Izvestiya Rossiiskoi Akademii Nauk, Seriya Geograficheskaya*. 2015, 5, 54–68 (in Russian). doi:10.15356/0373-2444-2015-5-54-68
27. Rérolle V., Ruiz-Pino D., Rafizadeh M. et al. Measuring pH in the Arctic Ocean: Colorimetric method or SeaFET? *Methods in Oceanography*. 2016, 17, 32–49. doi:10.1016/j.mio.2016.05.006
28. Copernicus Marine Environment Monitoring Service: Global ocean biogeochemistry hindcast dataset (GLOBAL_MULTIYEAR_BGC_001_029). URL: https://data.marine.copernicus.eu/product/GLOBAL_MULTIYEAR_BGC_001_029/ (дата обращения: 21.02.2023). doi:10.48670/moi-00019
29. Earth System Grid Federation portal. URL: <https://esgf-node.llnl.gov> (дата обращения: 03.03.2023).
30. O'Neill B.C., Tebaldi C., Van Vuuren D.P. et al. The scenario model intercomparison project (ScenarioMIP) for CMIP6. *Geoscientific Model Development*. 2016, 9(9), 3461–3482. doi:10.5194/gmd-9-3461-2016
31. Masson-Delmotte V., Zhai P., Pirani A. et al. (eds.). IPCC, 2021: Climate change 2021: The physical science basis. Contribution of working group I to the sixth assessment report of the intergovernmental panel on climate change. *Cambridge, Cambridge University Press*, 2023. doi:10.1017/9781009157896
32. Gnatiuk N., Radchenko I., Davy R., Morozov E., Bobylev L. Simulation of factors affecting *Emiliania huxleyi* blooms in Arctic and sub-Arctic seas by CMIP5 climate models: model validation and selection. *Biogeosciences*. 2020, 17(4), 1199–1212. doi:10.5194/bg-17-1199-2020

Литература

1. Doney S.C., Fabry V.J., Feely R.A., Kleypas J.A. Ocean acidification: The other CO₂ problem // *Annual Review of Marine Science*. 2009. Vol. 1. P. 169–192. doi:10.1146/annurev.marine.010908.163834
2. Xue L., Cai W.-J. Total alkalinity minus dissolved inorganic carbon as a proxy for deciphering ocean acidification mechanisms // *Marine Chemistry*. 2020. Vol. 222, N 103791. doi:10.1016/j.marchem.2020.103791
3. Mostofa K.M.G., Liu C.-Q., Zhai W. et al. Reviews and syntheses: Ocean acidification and its potential impacts on marine ecosystems // *Biogeosciences*. 2016. Vol. 13. P. 1767–1786. doi:10.5194/bg-13-1767-2016
4. Feely R.A., Doney S.C., Cooley S.R. Ocean acidification: Present conditions and future Changes in a high-CO₂ world // *Oceanography*. 2009. Vol. 22, N 4. P. 36–47. doi:10.5670/oceanog.2009.95

5. *Salisbury J., Green M.L., Hunt C.W., Campbell J.W.* Coastal acidification by rivers: A threat to shellfish? // *Eos, Transactions American Geophysical Union*. 2008. Vol. 89, N 50. P. 513. doi:10.1029/2008EO500001
6. *Yamamoto A., Kawamiya M., Ishida A., Yamanaka Y., Watanabe S.* Impact of rapid sea-ice reduction in the Arctic Ocean on the rate of ocean acidification // *Biogeosciences*. 2012. Vol. 9. P. 2365–2375. doi:10.5194/bg-9-2365-2012
7. *Yang X., Xue L., Li Y. et al.* Treated wastewater changes the export of dissolved inorganic carbon and its isotopic composition and leads to acidification in coastal oceans // *Environmental Science and Technology*. 2018. Vol. 52, N 10. P. 5590–5599. doi:10.1021/acs.est.8b00273
8. *Capelle D.W., Kuzyk Z.A., Papakyriakou T. et al.* Effect of terrestrial organic matter on ocean acidification and CO₂ flux in an Arctic shelf sea // *Progress in Oceanography*. 2020. Vol. 185, N 102319. doi:10.1016/j.pocean.2020.102319
9. *Keeling R.F., Körtzinger A., Gruber N.* Ocean deoxygenation in a warming world // *Annual Review of Marine Science*. 2010. Vol. 2, N 1. P. 199–229. doi:10.1146/annurev.marine.010908.163855
10. *Oschlies A., Brandt P., Stramma L., Schmidtko S.* Drivers and mechanisms of ocean deoxygenation // *Nature Geoscience*. 2018. Vol. 11, N 7. P. 467–473. doi:10.1038/s41561-018-0152-2
11. *Riebesell U., Zondervan I., Rost B. et al.* Reduced calcification of marine plankton in response to increased atmospheric CO₂ // *Nature*. 2000. Vol. 407. P. 364–367. doi:10.1038/35030078
12. *Albright R., Caldeira L., Hofelt J. et al.* Reversal of ocean acidification enhances net coral reef calcification // *Nature*. 2016. Vol. 531. P. 362–365. doi:10.1038/nature17155
13. *Pörtner H.-O.* Ecosystem effects of ocean acidification in times of ocean warming: A physiologists view // *Marine Ecology Progress Series*. 2008. Vol. 373. P. 203–217. doi:10.3354/meps07768
14. *Kwiatkowski L., Torres O., Bopp L. et al.* Twenty-first century ocean warming, acidification, deoxygenation, and upper-ocean nutrient and primary production decline from CMIP6 model projections // *Biogeosciences*. 2020. Vol. 17. P. 3439–3470. doi:10.5194/bg-17-3439-2020
15. *Zachos J.C., Röhl U., Schellenberg S.A. et al.* Rapid acidification of the ocean during the paleocene-eocene thermal maximum // *Science*. 2005. Vol. 308, N 5728. P. 1611–1615. doi:10.1126/science.1109004
16. *Zeebe R.E., Ridgwell A.* Past changes in ocean carbonate chemistry // *Ocean Acidification*, Ed. by Gattuso J.-P. and Hansson L. Oxford University Press, Oxford, 2011. P. 21–40. doi:10.1093/oso/9780199591091.003.0007
17. *Raven J., Caldeira K., Elderfield H. et al.* Ocean acidification due to increasing atmospheric carbon dioxide. The Royal Society, London, UK, 2005. 68 p.
18. *Jiang Z., Song Z., Bai Y. et al.* Remote sensing of Global sea surface pH based on massive underway data and machine learning // *Remote Sensing*. 2022. Vol. 14, N 10:2366. doi:10.3390/rs14102366
19. *Bindoff N.L., Willebrand J., Artale V. et al.* Observations: oceanic climate change and sea level. // *Climate change 2007: the physical science basis. Contribution of Working Group I / Ed. by: Solomon S., Qin D., Manning M., Chen Z., Marquis M., Averyt K.B., Tignor M., Miller H.L.*, Cambridge University Press, Cambridge, 2007. P. 385–428.
20. *Sabine C.L., Feely R.A., Gruber N. et al.* The oceanic sink for anthropogenic CO₂ // *Science American Association for the Advancement of Science (AAAS)*. 2004. Vol. 305, N5682. P. 367–371. doi:10.1126/science.1097403
21. *Orr J.C., Fabry V.J., Aumont O. et al.* Anthropogenic ocean acidification over the twenty-first century and its impact on calcifying organisms // *Nature*. 2005. Vol. 437. P. 681–686. doi:10.1038/nature04095
22. *Bellerby R., Anderson L., Osborne E. et al.* Arctic Ocean acidification: an update // *AMAP Assessment 2018: Arctic Ocean Acidification*. Arctic Monitoring and Assessment Programme (AMAP), Tromsø, Norway, 2018. 187 p. doi:10.25607/OBP-783
23. *Will S.* The Arctic in an Earth system context: From brake to accelerator of change // *Ambio*. 2006. Vol. 35, N 4. P. 153–159.
24. *Lauvset S.K., Lange N., Tanhua T. et al.* Global ocean data analysis project version 2.2021 (GLODAPv2.2021) (NCEI Accession 0237935). NOAA National Centers for Environmental Information. Dataset. 2021. URL: <https://www.ncei.noaa.gov/access/metadata/landing-page/bin/iso?id=gov.noaa.nodc:0237935> (дата обращения: 26.02.2023). doi:10.25921/ttgq-n825
25. *Артёмьев В.Е.* Геохимия органического вещества в системе река — море. М.: Наука, 1993. 204 с.
26. *Смирнов М.П.* Растворенные органические вещества и минерализация речных вод гор с тундрово-таежными типами вертикальной поясности России // *Известия Российской академии наук. Серия географическая*. 2015. № 5. С. 54–68. doi:10.15356/0373-2444-2015-5-54-68
27. *Rérolle V., Ruiz-Pino D., Rafizadeh M. et al.* Measuring pH in the Arctic Ocean: Colorimetric method or SeaFET? // *Methods in Oceanography*. 2016. Vol. 17. P. 32–49. doi:10.1016/j.mio.2016.05.006
28. Copernicus Marine Environment Monitoring Service: Global ocean biogeochemistry hindcast dataset (GLOBAL_MULTIYEAR_BGC_001_029). URL: https://data.marine.copernicus.eu/product/GLOBAL_MULTIYEAR_BGC_001_029/ (дата обращения: 21.02.2023). doi:10.48670/moi-00019
29. Earth system grid federation portal. URL: <https://esgf-node.llnl.gov> (дата обращения: 03.03.2023).

Malysheva A.S., Radchenko I.V., Pozdnyakov D.V.
Мальшева А.С., Радченко Ю.В., Поздняков Д.В.

30. *O'Neill B.C., Tebaldi C., Van Vuuren D.P.* et al. The scenario model intercomparison project (ScenarioMIP) for CMIP6 // Geoscientific Model Development. 2016. Vol. 9(9). P. 3461–3482. doi:10.5194/gmd-9-3461-2016
31. *Masson-Delmotte V., Zhai P., Pirani A.* et al. (eds.). IPCC, 2021: Climate Change 2021: The physical science basis. Contribution of working group I to the sixth assessment report of the intergovernmental panel on climate change. Cambridge: Cambridge University Press, 2023. doi:10.1017/9781009157896
32. *Gnatiuk N., Radchenko I., Davy R., Morozov E., Bobylev L.* Simulation of factors affecting *Emiliana huxleyi* blooms in Arctic and sub-Arctic seas by CMIP5 climate models: model validation and selection // Biogeosciences. 2020. Vol. 17(4). P. 1199–1212. doi:10.5194/bg-17-1199-2020

About the Authors

MALYSHEVA, Aleksandra S., РИНЦ AuthorID: 1120098, ORCID ID: 0009-0000-1225-9579,
WoS ResearcherID HPE-0124-2023, alexandra.malysheva@niersc.spb.ru

RADCHENKO, Iuliia V., Cand.Sc. (Agriculture), РИНЦ AuthorID: 1064639, ORCID ID: 0000-0002-8290-5043,
Scopus AuthorID: 56480302400, WoS ResearcherID AAF-4852-2019, yulia.rad@gmail.com

POZDNYAKOV, Dmitry V., Dr. Sc. (Phys.-Math.), РИНЦ AuthorID: 179336, ORCID ID: 0000-0003-0889-7855,
Scopus AuthorID: 56370460300, d.pozdnyakov@spbu.ru